Universal Critical Behavior of Curvature-Dependent Interfacial Tension

Subir K. Das[1,2] and Kurt Binder[2]

[1]*Theoretical Sciences Unit, Jawaharlal Nehru Centre for Advanced Scientific Research, Jakkur P.O., Bangalore 560064, India*
[2]*Institut für Physik, Johannes Gutenberg-Universität, Staudinger Weg 7, D-55099 Mainz, Germany*

From the analysis of Monte Carlo simulations of a binary Lennard-Jones mixture in the coexistence region, we provide evidence that the curvature dependence of the interfacial tension can be described by a simple theoretical function $\sigma(R)\xi^2 = C_1/[1 + C_2(\xi/R)^2]$, where ξ is the correlation length and R is the droplet radius. The universal constants C_1 and C_2 are estimated. In the model, a Tolman length is strictly absent, but, since its critical behavior is believed to be much weaker than ξ, we argue that it only provides a correction to scaling and does not affect the leading critical behavior, which should be described by the above function for any system in the Ising universality class. The large value of $C_2 \simeq 32$ implies that conventional nucleation theory becomes inaccurate even for a significantly large droplet radius.

Introduction.—Curved interfaces between coexisting phases are ubiquitous in nature [1–6]. E.g., in nanoscopic systems, for a wide range of compositions of different species, the minority component will exhibit a droplet structure with a well-defined radius of curvature R. Curved interfaces can also be seen in nanoscopic slit pores or cylindrical pores in wetting and drying phenomena. Such phase coexistence in porous media has widespread technological applications ranging from oil recovery to devices in nano- and microfluidics [5,6]. Quite naturally, understanding the properties of curved surfaces is of immense importance and indeed a longstanding difficult problem, particularly when one considers nucleation phenomena [1,2].

A central problem in this context is the understanding of the curvature dependence of the interfacial tension $\sigma(R)$ in the vicinity of a critical point. (Only near criticality can a continuum description of $\sigma(R)$ work, since far below criticality the critical nucleus contains only of the order of 100 molecules and nonuniversal details matter). The critical behavior of flat ($R \to \infty$) interfacial tension is rather well-studied [7,8], its singularity as a function of the reduced temperature t [$= (T_c - T)/T_c$, T_c being the critical temperature] being

$$\sigma(\infty) \equiv \sigma \approx \sigma_0 t^{2\nu} \tag{1}$$

in three spatial dimensions (d). In Eq. (1), ν is the exponent for the correlation length ξ:

$$\xi \approx \xi_0^- t^{-\nu}, \tag{2}$$

where ξ_0^- is the critical amplitude when T_c is approached from below and the $3 - d$ Ising universality value for ν is $\simeq 0.63$. However, related knowledge about $\sigma(R)$ [9–13] is rather poor.

Traditionally, it has been assumed that, to the leading-order correction, $\sigma(R)$ has the form [9]

$$\sigma(R) \simeq \frac{\sigma(\infty)}{1 + 2\frac{\delta}{R}}, \tag{3}$$

where δ is referred to as the Tolman length. Physically, δ is interpreted as the separation between the equimolar surface and the surface of tension [10]. Recently [13], it has been argued that the critical singularity of δ can be described as ($\beta \simeq 0.325$ being the order parameter exponent and δ_0 a critical amplitude)

$$\delta \approx \delta_0 t^{-(\nu-\beta)}. \tag{4}$$

On the other hand, there is evidence [12] that δ is very small (which corresponds to a very small value for δ_0), of the order of 10% of intermolecular distances, only about 30% below T_c. Thus, the practical relevance of Eq. (3) is somewhat uncertain, even though the value of δ_0 could be larger for a highly asymmetric system [13(c)].

While, in general, the equimolar surface and the surface of tension are expected to be different, for models having Ising-like up-down symmetry, they should coincide, so that $\delta = 0$. For such symmetric cases, of course, it is natural to write [11,12]

$$\sigma(R) \simeq \frac{\sigma(\infty)}{1 + 2(\frac{\ell}{R})^2}, \qquad R \to \infty, \tag{5}$$

where ℓ is a parameter that also has the dimension of length. In this Letter, we address the validity of Eq. (5) by using a phase-separating symmetric binary mixture. Further, the critical behavior of the length ℓ is investigated. A knowledge of the latter, combined with the universal critical amplitude ratios, allows us to empirically construct a universal scaling function for the critical behavior of $\sigma(R)$ containing universal constants. We expect this universality to be valid even for asymmetric situations where $\delta \neq 0$, since the divergence of ℓ is much stronger than that of δ. We also discuss the consequence of our findings in the

context of nucleation barriers, which are of direct experimental relevance.

  Model and method.—We employ a $3 - d$ binary $(A + B)$ fluid model where particles at positions $\vec{r}_i$ and $\vec{r}_j$, confined in a periodic box of volume V $(= L^3)$, interact via

$$u(r = |\vec{r}_i - \vec{r}_j|) = U(r) - U(r_c) - (r - r_c)\frac{dU}{dr}\Big|_{r=r_c}, \quad (6)$$

within a distance $r < r_c$. In Eq. (6), $U(r)$ is the standard (12, 6) Lennard-Jones potential with pairwise interaction strength $\epsilon_{AA} = \epsilon_{BB} = 2\epsilon_{AB} = \epsilon$ and interparticle diameter $d_{AA} = d_{BB} = d_{AB} = d_0$. This choice yields an Ising-like perfectly symmetric model that exhibits a liquid-liquid transition. We study the system at a high density $\rho = Nd_0^3/V = 1.0$ ($N = N_A + N_B$, N_α being the number of particles of species α) so that there is no coupling between liquid-liquid and gas-liquid transitions, and the temperature range is chosen such that crystallization does not occur. The cutoff distance r_c is set to $2.5d_0$; further, ϵ, k_B, and d_0 are set to unity. The phase behavior (with $T_c \simeq 1.423$) for this model is well-studied [14–16]. With respect to its critical behavior, it is a prototype of the Ising universality class, describing critical phenomena in systems such as anisotropic magnets, mixtures, and the liquid-vapor transition.

  We adopt an efficient successive umbrella-sampling [17] Monte Carlo [18] method in the semigrand canonical [19] ensemble. This allows us to sample the probability distribution $P(x_A)$ as a function of concentration x_A of A particles. $P(x_A)$ has a double peak structure in the two-phase region, the locations of the peaks giving points on the A-rich or B-rich branches of the coexistence curve. The concentration-dependent effective free energy density, relative to the value at the bulk coexistence, can be obtained as

$$f_L(x_A; T) = -\frac{k_B T}{V}\ln[P(x_A)/P(x_A^{\text{coex}})], \quad (7)$$

an example of which is shown in Fig. 1(a). There, the minimum on the left-hand side corresponds to a pure B-rich phase at the bulk coexistence composition. Gradually, with the increase of x_A, at a supersaturated concentration, marked by an arrow, a spherical droplet of the A-rich phase nucleates (marking the evaporation-condensation transition) in the background of the B-rich phase. The size of this droplet increases as one moves further before a cylindrical droplet becomes more stable at a higher concentration, marked by another arrow. Finally, close to the critical concentration ($x_A = 1/2$), one obtains a slab geometry. The flat part of the free energy (f_{hump}) corresponds to the excess surface free energy density due to two flat interfaces in the slab, which allows us to calculate the L-dependent flat interfacial tension [20] as
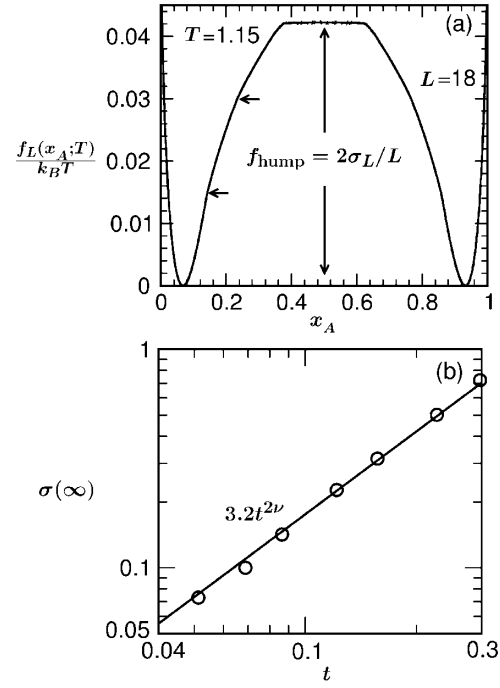

FIG. 1. (a) Plot of effective free energy density $f_L(x_A; T)$ vs x_A at $T = 1.15$ for $L = 18$. The left arrows mark, respectively, the evaporation-condensation transition and a transition from spherical droplet to cylindrical droplet structure. (b) Plot of $\sigma(\infty)$ vs t on a log scale. The solid line corresponds to $3.2t^{2\nu}$.

$\sigma_L = L f_{\text{hump}}/2$. An appropriate finite-size scaling analysis [18,21] of σ_L then gives us $\sigma(\infty)$.

  To obtain $\sigma(R)$, we focus on the part of f_L where a spherical droplet is stable and use the principle that the coexisting phases have equal chemical potential. So, the task [22] here then is to identify the pure A-rich and B-rich phases having the same chemical potential as the system where a spherical A-rich droplet is embedded in the sea of the B-rich phase. Then, the bulk contribution of the free energy can be read out, and subtraction of this from the total would give the excess part coming from the curved interface. The identification of the concentrations corresponding to the pure phases having the same chemical potential as the one containing a droplet could easily be done from the derivative of f_L that gives us chemical potentials relative to the bulk coexistence concentration as

$$\frac{1}{k_B T}\Delta\mu(x_A, T) = \left(\frac{\partial f_L(x_A, T)}{\partial x_A}\right)_T. \quad (8)$$

  Results.—The critical behavior of $\sigma(\infty)$, calculated from the method demonstrated in Fig. 1(a), is studied in Fig. 1(b), where it is plotted vs t on a log scale. The continuous line there is a fit to Eq. (1). The data are quite consistent with the expectation, and we obtain the amplitude (in Lennard-Jones units) $\sigma_0 = 3.2$.

  With the expectation that, for the symmetric model studied here, $\delta = 0$, in Fig. 2, we plot $\frac{\sigma(\infty)}{\sigma(R)} - 1$ as a function
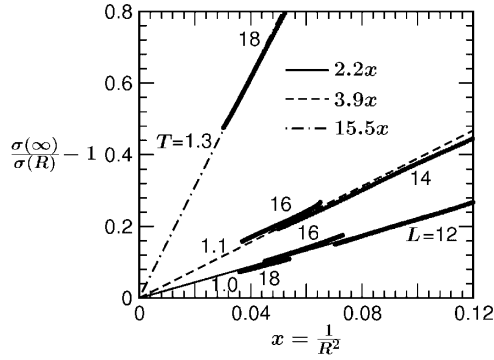
FIG. 2. Plots of $\frac{\sigma(\infty)}{\sigma(R)} - 1$ vs $1/R^2$ for different system sizes at three temperatures. The various straight lines are fits to the data sets.

of $1/R^2$. Indeed, the linear behaviors for all temperatures confirm the validity of Eq. (5). Ideally, of course, the data for $\sigma(R)$ from different system sizes L (as indicated next to the thick lines), at a particular temperature, should superimpose on a single curve. However, the scatter for different L values is due to residual statistical error. Various thin straight lines in this graph are fits to the simulation data, from the slopes of which we obtain ℓ as a function of temperature.

In Fig. 3, we plot ℓ as a function of t, on a log scale. The continuous line there has a power-law form with the Ising value of the critical exponent for ξ, with an amplitude $\ell_0 \simeq 0.6$. The very nice agreement of the simulation result with the solid line, at temperatures closer to T_c, strongly indicates that ℓ diverges at criticality, mirroring the behavior of ξ. The deviation of the simulation results from the solid line, starting from about 15% below T_c, is due to corrections to scaling and is consistent with other studies of critical phenomena. However, for a more quantitative statement, calculation of ξ is in order. This we do by assuming an Ornstein-Zernike form, $S_{cc}(q;T) \simeq k_B T \chi/(1 + q^2 \xi^2)$, of the relevant concentration-concentration structure factor, for wave vector $q \to 0$ and using the values of
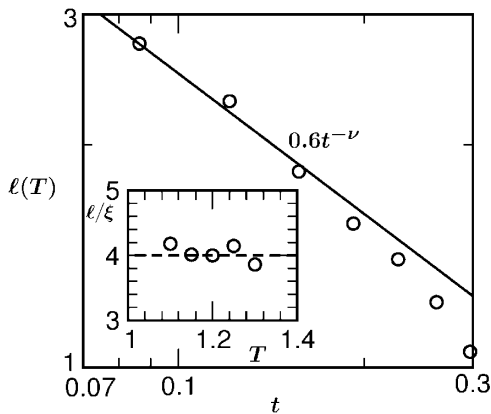

FIG. 3. Plot of ℓ vs t on a log scale. The solid line corresponds to $0.6 t^{-\nu}$. The inset shows a plot of ℓ/ξ as a function of temperature.

$k_B T \chi$ obtained from probability distribution $P(x_A)$ as $k_B T \chi = N(\langle x_A^2 \rangle - \langle x_A \rangle^2)$. In the inset of Fig. 3, we show the ratio ℓ/ξ, which is seen to remain constant at a value $\simeq 4$ over a wide range of temperatures. This provides the critical amplitude $\xi_0^- \simeq 0.15$. The knowledge of σ_0 and ξ_0^- then gives us the value of the universal constant, $\omega = [4\pi\sigma_0(\xi_0^-)^2]^{-1} \simeq 1.1$. While this value is consistent with an earlier Monte Carlo simulation of a different system [23], the most recent estimate of ω is $\simeq 0.87$ [24,25]. In view of the fact that we do not have data closer than 5% to T_c, such a discrepancy is expected.

Using our estimate that $\ell = 4\xi$, from Eq. (5), we obtain a form for the critical behavior of $\sigma(R)$ as

$$\sigma(R)\xi^2 = \frac{C_1}{1 + C_2 (\frac{\xi}{R})^2}, \tag{9}$$

where $C_1 = \sigma_0(\xi_0^-)^2 = 1/4\pi\omega$, which is thus a universal constant, namely, [24,25] $\simeq 0.089$, whereas, using the simulation values of σ_0 and ξ_0^-, we obtain $\simeq 0.075$. While we obtain $C_2 = 32$ by taking $\ell/\xi = 4$, it needs to be checked whether our estimate for this universal constant is accurate. On the other hand, considering the fact that this second-order term is also present in an asymmetric model and the critical divergence of ℓ is significantly stronger than δ, the first-order correction in $1/R$ can be treated merely as a correction to scaling in the critical vicinity. Equation (9) then is a universal form for the critical behavior of $\sigma(R)$, irrespective of whether the system is symmetric or not. Thus, we propose that Eq. (9) also holds for the vapor-liquid transition in an asymmetrical model in the critical region.

In Fig. 4, we plot $\sigma(R)/\sigma(\infty)$ as a function of the scaling variable R/ξ. The continuous line there corresponds to
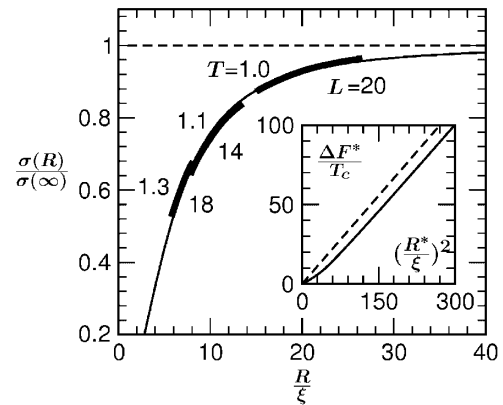

FIG. 4. Plot of $\sigma(R)/\sigma(\infty)$ vs R/ξ. The continuous line is the theoretical form (9), which is compared with the simulation data (for $T = 1.0$, we have obtained ξ from the relation $\ell/\xi = 4$ due to difficulty in getting ξ at such a low temperature from the Ornstein-Zernike relation) represented by thicker lines. The horizontal dashed line corresponds to the CNT. The inset shows a plot of $\frac{\Delta F^*}{T_c}$ vs $(R^*/\xi)^2$, demonstrating the (significant) reduction of the nucleation barrier compared to the CNT (dashed straight line).

Eq. (9), while the thicker lines are representative simulation results from various system sizes at three different temperatures. The agreement between Eq. (9) and the simulation is remarkable. This should be compared with the dashed line corresponding to the classical nucleation theory (CNT) failure, which looks quite prominent even for very large values of R/ξ. A consequence of the curvature-dependent surface tension is illustrated in the inset of this figure in the context of the nucleation barrier ΔF^*. For the latter, we obtained the form

$$\frac{\Delta F^*}{T_c} \simeq 0.37 \frac{y^2}{C_2 + y}; \qquad y = \left(\frac{R^*}{\xi}\right)^2, \qquad (10)$$

where R^* is the size of a critical nucleus. Again, in this plot, the dashed line stands for the CNT while the continuous line corresponds to Eq. (10). Because of the large value of $C_2 \simeq 32$, the CNT is expected to be accurate only for very large values of y. Note that, even though the idea of a universal scaling function for the nucleation barriers in the critical region is not new [26], an explicit estimate is given for the first time.

Summary.—We have studied the curvature-dependent interfacial tension in a symmetric binary Lennard-Jones fluid via a successive umbrella-sampling Monte Carlo method. The analysis of the results, by using a recently developed powerful method, shows that the leading-order correction to $\sigma(R)$ is quadratic in $1/R$; thus, a Tolman length is absent. The critical behavior of the length ℓ, defined in Eq. (5), is proportional to the correlation length, which has a much stronger divergence than the one of the Tolman length δ. We propose a scaling form for the critical behavior of $\sigma(R)$ containing universal constants. While the Tolman length would only provide a nonuniversal correction to scaling, this form is expected to be universal for both symmetric and asymmetric situations. We have also discussed the consequence of this curvature dependence in the context of the nucleation barrier. It is pointed out that the classical nucleation theory fails even for a very large droplet radius. These results are of great experimental significance. While existing studies near T_c (e.g., [27,28]) have only addressed the combined effects of nucleation and growth, as discussed in [26], an extension of a recent technique that directly yields the nucleation rate only [29] to the critical region should be illuminating.

[1] F. F. Abraham, *Homogeneous Nucleation Theory* (Academic, New York, 1974).
[2] K. Binder, Rep. Prog. Phys. **50**, 783 (1987).
[3] P. G. de Gennes, Rev. Mod. Phys. **57**, 827 (1985).
[4] D. Bonn and D. Ross, Rep. Prog. Phys. **64**, 1085 (2001).
[5] *Handbook of Porous Solids*, edited by F. Schüth, K. S. W. Sing, and J. Weitkamp (Wiley-VCH, Weinheim, 2002).
[6] T. M. Squires and S. R. Quake, Rev. Mod. Phys. **77**, 977 (2005).
[7] K. Binder and E. Luijten, Phys. Rep. **344**, 179 (2001).
[8] V. Privman *et al.*, in *Phase Transitions and Critical Phenomena*, edited by C. Domb and J. L. Lebowitz (Academic, New York, 1991), Vol. 14, Chap. 1.
[9] R. C. Tolman, J. Chem. Phys. **16**, 758 (1948); **17**, 118 (1949); **17**, 333 (1949).
[10] J. S. Rowlinson, J. Phys. Condens. Matter **6**, A1 (1994).
[11] M. P. A. Fisher and M. Wortis, Phys. Rev. B **29**, 6252 (1984).
[12] B. J. Block, S. K. Das, M. Oettel, P. Virnau, and K. Binder, J. Chem. Phys. **133**, 154702 (2010).
[13] (a) M. A. Anisimov, Phys. Rev. Lett. **98**, 035702 (2007); (b) C. E. Bertrand and M. A. Anisimov, Phys. Rev. Lett. **104**, 205702 (2010); (c) M. A. Anisimov and H. J. St. Pierre, Phys. Rev. E **78**, 011105 (2008).
[14] S. K. Das, J. Horbach, K. Binder, M. E. Fisher, and J. V. Sengers, J. Chem. Phys. **125**, 024506 (2006).
[15] S. K. Das, M. E. Fisher, J. V. Sengers, J. Horbach, and K. Binder, Phys. Rev. Lett. **97**, 025702 (2006).
[16] S. Roy and S. K. Das, Europhys. Lett. **94**, 36001 (2011).
[17] P. Virnau and M. Müller, J. Chem. Phys. **120**, 10925 (2004).
[18] D. P. Landau and K. Binder, *A Guide to Monte Carlo Simulations in Statistical Physics* (Cambridge University Press, Cambridge, England, 2009), 3rd ed.
[19] K. Binder *et al.*, Acta Metall. **29**, 1655 (1981).
[20] K. Binder, Phys. Rev. A **25**, 1699 (1982).
[21] M. E. Fisher, in *Critical Phenomena*, edited by M. S. Green (Academic, London, 1971), p. 1; M. E. Fisher and M. N. Barber, Phys. Rev. Lett. **28**, 1516 (1972).
[22] M. Schrader, P. Virnau, and K. Binder, Phys. Rev. E **79**, 061104 (2009).
[23] K. K. Mon and D. Jasnow, Phys. Rev. A **30**, 670 (1984).
[24] M. E. Fisher and H. Wen, Phys. Rev. Lett. **68**, 3654 (1992).
[25] M. Hasenbusch and K. Pinn, Physica (Amsterdam) **192A**, 342 (1993).
[26] K. Binder and D. Stauffer, Adv. Phys. **25**, 343 (1976) [Eqs (5.15) and (5.19)].
[27] D. Dahl and M. R. Moldover, Phys. Rev. Lett. **27**, 1421 (1971).
[28] J. S. Huang and W. I. Goldburg, Phys. Rev. Lett. **34**, 639 (1975).
[29] A. Fladerer and R. Strey, J. Chem. Phys. **124**, 164710 (2006).